HAL
open science

Rainfall-runoff modelling in a catchment with a complex groundwater flow system: application of the Representative Elementary Watershed (REW) approach

G. P. Zhang, H. H. G. Savenije

To cite this version:

G. P. Zhang, H. H. G. Savenije. Rainfall-runoff modelling in a catchment with a complex groundwater flow system: application of the Representative Elementary Watershed (REW) approach. Hydrology and Earth System Sciences Discussions, 2005, 2 (3), pp.639-690. hal-00298641

HAL Id: hal-00298641

https://hal.science/hal-00298641v1

Submitted on 18 Jun 2008

HAL is a multi-disciplinary open access archive for the deposit and dissemination of scientific research documents, whether they are published or not. The documents may come from teaching and research institutions in France or abroad, or from public or private research centers.

L'archive ouverte pluridisciplinaire **HAL**, est destinée au dépôt et à la diffusion de documents scientifiques de niveau recherche, publiés ou non, émanant des établissements d'enseignement et de recherche français ou étrangers, des laboratoires publics ou privés.

Hydrol. Earth Sys. Sci. Discuss., 2, 639–690, 2005
www.copernicus.org/EGU/hess/hessd/2/639/
SRef-ID: 1812-2116/hessd/2005-2-639
European Geosciences Union

Hydrology and Earth System Sciences Discussions

Rainfall-runoff modelling in a catchment with a complex groundwater flow system: application of the Representative Elementary Watershed (REW) approach

G. P. Zhang and H. H. G. Savenije

Water Resources Section, Faculty of Civil Engineering and Applied Geosciences, Delft University of Technology, Stevinweg 1, P.O. Box 5048, 2600 GA Delft, The Netherlands

Received: 7 March 2005 – Accepted: 15 April 2005 – Published: 12 May 2005

Correspondence to: G. P. Zhang (g.p.zhang@citg.tudelft.nl)

© 2005 Author(s). This work is licensed under a Creative Commons License.

Abstract

Based on the Representative Elementary Watershed (REW) approach, the modelling tool REWASH (Representative Elementary WAterShed Hydrology) has been developed and applied to the Geer river basin. REWASH is deterministic, semi-distributed, physically based and can be directly applied to the watershed scale. In applying REWASH, the river basin is divided into a number of sub-watersheds, so called REWs, according to the Strahler order of the river network. REWASH describes the dominant hydrological processes, i.e. subsurface flow in the unsaturated and saturated domains, and overland flow by the saturation-excess and infiltration-excess mechanisms. Through flux exchanges among the different spatial domains of the REW, surface and subsurface water interactions are fully coupled. REWASH is a parsimonious tool for modelling watershed hydrological response. However, it can be modified to include more components to simulate specific processes when applied to a specific river basin where such processes are observed or considered to be dominant. In this study, we have added a new component to simulate interception using a simple parametric approach. Interception plays an important role in the water balance of a watershed although it is often disregarded. In addition, a refinement for the transpiration in the unsaturated zone has been made. Finally, an improved approach for simulating saturation overland flow by relating the variable source area to both the topography and the groundwater level is presented. The model has been calibrated and verified using a 4-year data set, which has been split into two for calibration and validation. The model performance has been assessed by multi-criteria evaluation. This work is the first full application of the REW approach to watershed rainfall-runoff modelling in a real watershed. The results demonstrate that the REW approach provides an alternative blueprint for physically based hydrological modelling.

1. Introduction

Hydrological models are important and necessary tools for water and environmental resources management. Demands from society on the predictive capabilities of such models are becoming higher and higher, leading to the need of enhancing existing models and even of developing new theories. Existing hydrological models can be classified into three types, namely, 1) empirical models (black-box models); 2) conceptual models; and 3) physically based models. To address the question of how land use change and climate change affect hydrological (e.g. floods) and environmental (e.g. water quality) functioning, the model needs to contain an adequate description of the dominant physical processes.

Following the blueprint proposed by Freeze and Harlan (1969), a number of distributed and physically based models have been developed, among which the well-known SHE (Abbott et al., 1986a, b), MIKE SHE (Refsgaard and Storm, 1995), IHDM (Beven et al., 1987; Calver and Wood, 1995), and THALES (Grayson et al., 1992a) models. Although the physically based distributed models are supposed to offer a great potential and utility in predicting the effects of land-use change and the hydrological response of ungauged basins, considerable debate on both the advantages and disadvantages of such models (see, e.g., Beven 1989, 1996a, b, 2002; Grayson et al., 1992b; Refsgaard et al., 1996; O'Connell and Todini, 1996) has arisen along with the research and application of those models. In general, such models suffer from immense demands on data. They are time-consuming and parameter identification is extremely difficult, viz. the equifinality problem (Beven, 1993, 1996c; Savenije, 2001).

Conceptual models form by far the largest group of hydrological models that have been developed in the hydrological community and which are most often applied in operational practice. Among those are SAC-SMA (Burnash et al., 1973; Burnash, 1995), HBV (Bergström and Forsman, 1973; Bergström, 1995), and LASCAM (Sivapalan et al., 1996). Most conceptual models are spatially lumped, neglecting the spatial variability of the state variables and parameters. To improve the potential for making use

of spatially distributed data, some lumped conceptual models have been extended to be distributed or semi-distributed. Examples are the HBV-96 model (Lindström et al., 1997), TOPMODEL (Beven, 1995) and the ARNO model (Todini, 1996). Parameters of this type of models, however, are either lacking physical meaning or cannot be measured in the field.

In view of all these different types of modelling approaches, one can notice that there is no commonly accepted general framework for describing the hydrological response directly applicable at watershed scale. To fill in this gap, Reggiani et al. (1998, 1999) made an attempt to derive a unifying framework for modelling watershed response, which has been named the Representative Elementary Watershed (REW) approach. This theory applies global balance laws of mass and momentum and yields a system of coupled non-linear ordinary differential equations at the REW scale, governing flows between different sub-domains of a REW. To demonstrate the applicability of the REW approach, Reggiani et al. (2000) investigated the long-term water balance of a single hypothetical REW using the equations in non-dimensional form. In that work, only hillslope subsurface responses, i.e. flows in the unsaturated and saturated zones were considered. In succession, Reggiani et al. (2001) applied the REW approach to a natural watershed but only focusing on the response of the channel network. They provided the theoretical development of the REW approach and demonstrated that the approach can provide a framework for an alternative blueprint for modelling watershed response (Beven, 2002; Reggiani and Schellekens, 2003).

Parallel to theory formulation, much work has been done to apply the REW approach. Reggiani and Rientjes (2005), Zhang et al. (2003, 2004a, b) reported on advances of the research in this regard. However, it has been realised that the functional relationships for closing the balance equations can form a hindrance to a successful application (e.g. Beven, 2002). Zhang et al. (2005a) made a step towards a better model parameterisation and showed encouraging results when applied to a temperate humid watershed. One should note that an incomplete description of hydrological processes inevitably results in poor performance and leads to erroneous results. For instance, as

pointed out by Savenije (2004, 2005), neglecting interception can introduce significant errors in other parameters. Moreover, previous research on the REW approach has not shown a full application with convincing results. Therefore, this paper reports on the current state of development of the REW approach within our research framework.

In this work, the numerical model has been enhanced by the inclusion of interception and the modification of the transpiration scheme for the unsaturated zone. The model has been applied to the Geer river basin and the model performance has been evaluated through calibration and verification procedures. Model calibration and verification have been carried out through a combination of manual and automatic calibration, and a split-sample test. Sensitivity analysis has been performed to examine model behaviour and identify the most important parameters. Modelling results show that the hydrographs can be well reproduced and the model is able to simulate the watershed response at a large spatial scale in a lumped fashion while the parameters are kept physically meaningful. Results also show that the revised model performs better than the previous ones. This, on the other hand, indicates that further research on the REW approach is needed (e.g., Zhang et al., 2005b) accompanying the growth of our knowledge and understanding of real world hydrology. While the approach, as a general framework, provides a way towards a new generation of physically based models, we understand that the hydrological phenomenon and processes are watershed-specific.

2. Mathematical representation of the hydrological processes

2.1. The concept of the REW approach

In the REW approach, a river basin is spatially divided into a number of sub-watersheds, so-called REWs. The REW preserves the basic structure and functional components of a watershed (hill-slopes and channels, Fig. 1). The discretisation is based on the analysis of the basin topography using the Strahler stream order system. The topographical boundaries of REWs coincide with their surface water divides, thus

REWs are naturally interconnected through the stream networks as well as through the subsurface flow paths in terms of water flux exchanges. Each REW is defined in three dimensions and is delimited externally by a prismatic mantle.

The volumetric entities of a REW contain flow domains commonly encountered or described within a watershed: 1) the unsaturated flow domain, 2) the saturated flow domain, 3) the saturation-excess overland flow domain, 4) the concentrated overland flow domain (or the infiltration-excess overland flow domain), and 5) the river channel. These domains are characterised by different temporal scales. For instance, overland flow has a time scale of minutes to hours, while saturated groundwater flow has months to years (Blöschl and Sivapalan, 1995).

In the REW approach, up-scaled balance laws of mass and momentum for each flow domain were derived (Reggiani et al., 1998, 1999), resulting in a set of non-linear ordinary differential equations (ODEs) which no longer contain any spatial information below the REW scale. The general form of the ODEs reads:

$$\frac{\mathrm{d}\phi}{\mathrm{d}t} = \sum_i e_{\phi i} + s \tag{1}$$

where ϕ represents a generic thermodynamic property such as mass or momentum. $e_{\phi i}$stands for a generic exchange term of ϕ and s is a grouped sink/source term for the domain in question. This form can be extended to include terms for more complex flow phenomena, such as multi-phase flow and pollutants transport. In contrast to grid-based methods applied in most distributed model approaches (e.g. Abbott et al., 1986a, b), the REW approach uses the sub-watersheds (REWs) as “cells”, the basic discretisation units on which the ODEs are solved. After rigorous theoretical derivation, REW-scale equations for: Darcy’s law, Manning’s law, and the Saint-Venant equations have been obtained and employed in our model, which are valid for subsurface, overland and channel flow respectively.

2.2. Description of the improved model

In many hydrological models or model approaches, interception is neglected even though it is the first process in the chain of interlinked rainfall-runoff processes (Savenije, 2004). By ignoring this process, errors are introduced that propagate into the subsequent processes simulated (particularly into the soil moisture and groundwater flow process) and into the water balance regime in the different stocks of a watershed, although sometimes they may not be detected by only looking at the single integral output: the simulated stream discharge. In the initial stage of the development and application of the REW approach, interception was not explicitly considered. Bearing this in mind, we have added a component in this model using a simple parametric approach to account for the interception effect. In addition, in line with the work by Zhang et al. (2003, 2004a, b, 2005a), a refinement for sub-grid variability of soil properties in the soil column has been taken into account. Moreover, a new approach to determine the saturated overland area has been introduced. Based on these modifications, the water balance equations for the different flow domains and governing equations for the various flow processes are described below.

2.2.1. Water balance equations for flow domains

Mass conservation is the first principle ruling water flux exchanges in a watershed system. In accordance with observation and understanding of the flow processes in the terrestrial system, a REW is sub-discretised vertically into various flow domains. Figure 2 illustrates the schematised profile of a REW with the different flow domains, their geometric quantities and the water flux exchange terms. With reference to Fig. 2, the water balance equations for each flow domain are given as follows.

Infiltration-excess overland flow domain

$$\frac{\mathrm{d}S_c}{\mathrm{d}t} = e_{ctop} + e_{ca} + e_{cu} + e_{co} \tag{2}$$

where S_c is the storage of the infiltration-excess overland flow domain. The fluxes e_{ctop}, e_{ca}, e_{cu} and e_{co} are the rainfall on the surface of this zone, the evaporation from interception on this zone, the infiltration to the saturated zone and the transfer towards the saturation-excess flow domain respectively. Since we are applying this model approach to a humid temperate river basin where the saturation-excess flow is dominant, the infiltration-excess overland flow is negligible, thus e_{co} is kept zero.

Saturation excess overland flow domain

$$\frac{dS_o}{dt} = e_{otop} + e_{oa} + e_{os} + e_{or} + e_{oc} \tag{3}$$

where S_o is the storage of the saturation-excess overland flow domain. The fluxes e_{otop}, e_{oa}, e_{os}, e_{or} and e_{oc} are the rainfall on the surface of this zone, the evaporation from this zone, the exchange between this zone and the saturated flow zone, the transfer to the river channel, and the exchange between this zone and the infiltration-excess flow zone, respectively. For the same reason stated above, e_{oc} is ignored.

Unsaturated subsurface flow domain

$$\frac{dS_u}{dt} = e_{ua} + e_{uc} + e_{us} \tag{4}$$

where S_u is the storage of the unsaturated flow domain. The fluxes e_{ua}, e_{uc}, and e_{us} are the transpiration, the infiltration and the percolation.

Saturated subsurface flow domain

$$\frac{dS_s}{dt} = e_{su} + e_{so} + e_{sr} + e_{si} + e_{sa} \tag{5}$$

where S_s is the storage of the saturated flow domain. The fluxes e_{su} and e_{so} are the counterparts of e_{us} and e_{os} in Eqs. (3) and (4), respectively; e_{sr}, e_{si} and e_{sa} are the exchange between the saturated zone and river channel, the exchange with the

neighbouring REWs (if any) and the groundwater abstraction (if any).

River channel

$$\frac{dS_r}{dt} = e_{rtop} + e_{ra} + e_{rs} + e_{ro} + e_{rin} + e_{rout} \tag{6}$$

where S_r is the storage of the river channel segment within the REW under investigation. The fluxes e_{rtop}, e_{ra}, e_{rin} and e_{rout} are the rainfall on the channel water surface, the evaporation from the water surface, the water coming from upstream channel segment(s) and the flow out of the segment of the REW in question, respectively. The fluxes e_{rs}, e_{ro} are the counterparts of e_{sr} and e_{or} in Eqs. (3) and (5), respectively.

The functional relationships to quantify the flux terms presented in these equations are described in the following section.

2.2.2. Parameterised governing equations for rainfall-runoff processes

Rainfall input

The rainfall flux on a REW is partitioned into three portions in terms of the area that captures the rainfall. e_{ctop} is the rainfall flux to the infiltration-excess overland flow area; e_{otop} to the saturation overland flow area and e_{rtop} to the river channel. They are described by

$$\begin{cases} e_{ctop} = \rho i A \omega_c \\ e_{otop} = \rho i A \omega_o \\ e_{rtop} = \rho i l_r w_r \end{cases} \tag{7}$$

where ρ [ML^{-3}] is the water density; A [L^2] the horizontally projected surface area of the REW; i [LT^{-1}] the precipitation intensity. ω_c [-] and ω_o [-] are the infiltration-excess and the saturation-excess overland flow area fractions, respectively. l_r [L] and w_r [L] are the length and width of the channel.

Interception

We assume that interception is taking place in the infiltration-excess flow domain. Considering a storage capacity of the interception media (e.g. tree leaves, undergrowth, forest floor and surface) and assuming that the intercepted water will be eventually evaporated within a day, the interception flux is determined by

$$e_{ca} = \min(i, i_{dc})\, \rho A \omega_c \tag{8}$$

where e_{ca} is the interception flux and i_{dc} [LT^{-1}] is the daily interception threshold.

Infiltration

Similar to the approach of Reggiani et al. (2000), the infiltration capacity can be computed by

$$f = \frac{K_{su}}{\Lambda_u}\left(\frac{1}{2}y_u + h_c\right) \tag{9}$$

where f [LT^{-1}] is the infiltration capacity; K_{su} [LT^{-1}] the vertical saturated hydraulic conductivity of the unsaturated zone; Λ_u [L] the length over which the wetting front is reached; y_u [L] the averaged unsaturated zone depth; and h_c [L] the capillary pressure head, which is described using the Brooks and Corey (1964) soil water retention model:

$$h_c = \psi_b \left(\frac{\theta_u}{\varepsilon_u}\right)^{-1/\mu} \tag{10}$$

where ψ_b [L] is the air entry pressure head; θ_u [-] and ε_u [-] are the soil moisture content and the effective soil porosity of the unsaturated zone respectively; μ [-] is the soil pore size distribution index.

It is reasonable to assume that all rainfall reaching the ground surface infiltrates into the soil when it is climate controlled, i.e. the rainfall intensity is lower than the infiltration capacity. Consequently, the actual infiltration flux is estimated by

$$e_{cu} = \min\left[(i - i_{dc}), f\right] \rho \omega_c A \tag{11}$$

where e_{cu} is the flux exchange between the infiltration-excess overland flow zone and the unsaturated zone. ω_c [-] is the area fraction of the infiltration-excess overland flow zone, which is equal to the unsaturated zone area fraction. The remaining symbols are the same as in the above equations. The first term of the right-hand side in Eq. (11) calculates the effective rainfall intensity.

Evaporation/transpiration

$$\begin{cases} e_{ua} = \min\left[1.0, \left(2\frac{\theta_u}{\varepsilon_u}\right)\right]\left[e_p - \min(i, i_{dc})\right]\rho\omega_u A & \text{(for Uzone)} \\ e_{oa} = e_p \rho \omega_o A & \text{(for Ozone)} \\ e_{ra} = e_p \rho l_r w_r & \text{(for Rzone)} \end{cases} \tag{12}$$

where e_{ua}, e_{oa} and e_{ra} are the transpiration flux from the unsaturated zone to the atmosphere, the evaporation fluxes from the saturation overland flow zone and the river channel surface to the atmosphere respectively; e_p [LT^{-1}] is the potential evaporation.

Percolation/capillary rise:

$$e_{us} = \alpha_{us} \rho \omega_c A \frac{K_u}{y_u}\left[\left(\frac{1}{2} - \frac{\theta_u}{\varepsilon_u}\right) y_u + h_c\right] \tag{13}$$

where e_{us} is the percolation flux from the unsaturated zone to the saturated zone or the capillary rise from the saturated zone to the unsaturated zone. As an additional condition, percolation is set to take place only if θ_u is greater than the field capacity θ_f. α_{us} [-] is the scaling factor for this flux exchange term. K_u [LT^{-1}] is the effective hydraulic conductivity for the unsaturated zone, which is a function of the saturation (θ_u/ε_u) of the unsaturated zone. K_u can be determined by the following relationship in Brooks and Corey (1964) approach:

$$K_u = K_{su}\left(\frac{\theta_u}{\varepsilon_u}\right)^{\lambda} \tag{14}$$

$$\lambda = 3 + \frac{2}{\mu} \tag{15}$$

where λ is the soil pore-disconnectedness index.

Base flow:

$$e_{sr} = \frac{\rho K_{sr} l_r P_r}{\Lambda_r}(h_r - h_s) \tag{16}$$

where e_{sr} is the flux exchange between the saturated zone and the river channel. K_{sr}[LT^{-1}] and P_r [L] are the hydraulic conductivity for the river bed transition zone and the wetted perimeter of the river cross section, respectively. Λ_r [L] is the depth of transition layer of the river bed. h_r [L] and h_s [L] are the total hydraulic heads in the river channel and the saturated zone, respectively.

Exfiltration to the surface:

$$e_{so} = \frac{\rho K_{ss}\omega_o A}{\Lambda_s \cos\gamma_o}(h_s - h_o) \tag{17}$$

where e_{so} is the flux exchange between the saturated zone and the saturated overland flow zone (seepage face). K_{ss} [LT^{-1}] and ω_o [-] are the saturated hydraulic conductivity for the saturated zone and the area fraction of the saturated overland flow zone respectively. h_s [L] and h_o [L] are respectively the total hydraulic head in the saturated zone and the saturated overland flow zone. Λ_s [L] is a typical length over which the head difference between the saturated zone and the saturated overland zone is dissipated. γ_o is the average slope angle of the seepage face in radian.

Regional groundwater flow:

$$e_{si} = \alpha_{si}\rho\,(h_s - h_{si}) \tag{18}$$

where e_{si} is the flux exchange between the saturated zones of the REW in question and its ith neighbouring REW; h_s [L] and h_{si} [L] are the total hydraulic heads of the saturated zones of the two neighbouring REWs, respectively. α_{si} [L^2T^{-1}] is a lumped scaling factor involving the contour length of the mantle segment of the ith REW, the harmonic mean of the saturated hydraulic conductivity over the two REWs, etc. If there is no groundwater connection between REWs or if the groundwater level has a horizontal gradient at the water divide, then α_{si} is set to zero.

Lateral overland flow to channel:

$$e_{or} = 2\rho y_o l_r \frac{1}{n}(\sin\gamma_o)^{1/2}(y_o)^{2/3} \tag{19}$$

where e_{or} is the flux of the saturation overland flow to the channel segment within the REW. y_o [L] is the average depth of the flow sheet on the surface of the overland flow domain; and n [$TL^{-1/3}$] the Manning roughness coefficient.

Channel flow:

$$e_{rin} = \rho \sum_i \frac{1}{2} m_i \left(v_r + v_{ri}\right) \tag{20}$$

$$e_{rout} = \rho \frac{1}{2} m \left(v_r + v_{rj}\right) \tag{21}$$

$$v_r = \sqrt{\frac{8g}{P_r l_r \xi} \left[m_r l_r \sin \gamma_r + \sum_i \frac{1}{4} y_r \left(m_r + m_{ri}\right) - \frac{1}{4} y_r \left(m_r + m_{rj}\right) \right]} \tag{22}$$

where e_{rin} is the inflow flux from upstream channel segment(s), and e_{rout} is the outflow flux of the segment under study. m_r [L^2], m_{ri} [L^2] and m_{rj} [L^2] are the average cross-sectional area of the channel segment under study, of the ith inflow channel and of the outflow channel respectively; v_r [LT^{-1}], v_{ri} [LT^{-1}] and v_{rj} [LT^{-1}] are the flow velocities within the channel segment under study, and of the inflow and outflow channels respectively; ξ [-] is the average Darcy-Weisbach friction factor and g [LT^{-2}] is the gravitational acceleration; γ_r [-] is the average slope angle of the river channel and y_r [L] is the water depth of the channel under study.

2.2.3. Additional functional relationships for the closure of the water balance equations

Zhang et al. (2004b, 2005a) proposed an expression for the saturation overland flow area fraction, which has the following form:

$$\begin{cases} \omega_o = \alpha_{sf} \left(\frac{y_s + z_s - z_r}{z_{surf} - z_r} \right)^{tg\gamma_o} & (\text{if } y_s + z_s \geq z_r) \\ \omega_o = 0 \quad (\text{if } y_s + z_s < z_r) \end{cases} \tag{23}$$

Therefore,

$$\frac{d\omega_o}{dt} = \alpha_{sf} \frac{(y_s + z_s - z_r)^{tg\gamma_o - 1}}{(z_{surf} - z_r)^{tg\gamma_o}} tg\gamma_o \frac{dy_s}{dt} \quad (\text{if } y_s + z_s \geq z_r) \tag{24}$$

where α_{sf} [-] is a scaling factor, which can be estimated from the surface runoff coefficient taking into account the average groundwater level. y_s, z_s, z_r, z_{surf} and γ_o are the geometric quantities of a REW defined in Fig. 2.

There are a number of geometric relationships supplementary to the balance equations, among those:

$$\omega_o + \omega_c = 1 \tag{25}$$

$$y_u \omega_c + y_s = Z \tag{26}$$

where Z is the average soil depth of a REW. As a result,

$$\frac{d\omega_c}{dt} = -\frac{d\omega_o}{dt} \tag{27}$$

$$\frac{d}{dt}(y_u \omega_c) = -\frac{dy_s}{dt} \tag{28}$$

In Eq. (5), e_{sa} is the sink (groundwater abstraction) or source (artificial recharge) term, which can be calculated by

$$e_{sa} = \rho G A \tag{29}$$

where G [LT^{-1}] is the abstraction or recharge rate imposed on the REW in question.

Substituting Eqs. (7), (8), (9), (10), (11), (12), (13), (16), (17), (18), (19), (20), (21), (27), (28) and (29) into Eqs. (2), (3), (4), (5) and (6), we obtain the full water balance equations for a REW.

$$\frac{dy_c}{dt} = \underbrace{i}_{\text{rainfall}} - \underbrace{\min(i, i_{dc})}_{\text{interception}} - \underbrace{\min\left[(i - i_{dc}), \frac{K_{su}}{\Lambda_u}\left(\frac{1}{2}y_u + h_c\right)\right]}_{\text{infiltration}} + \underbrace{\frac{y_c}{1 - \omega_o}\frac{d\omega_o}{dt}}_{\text{area change}} \tag{30}$$

$$\frac{dy_o}{dt} = \underbrace{i}_{\text{rainfall}} - \underbrace{e_p}_{\text{evaporation}} + \underbrace{\frac{K_{ss}}{\Lambda_s \cos\gamma_o}(h_s - h_o)}_{\text{groundwater exfiltration}} - \underbrace{\frac{2y_o l_r}{A\omega_o}\frac{1}{n}(\sin\gamma_o)^{1/2}(y_o)^{2/3}}_{\text{overland flow to channel}} - \underbrace{\frac{y_o}{\omega_o}\frac{d\omega_o}{dt}}_{\text{area change}} \tag{31}$$

$$\frac{d\theta_u}{dt} = \underbrace{\min\left[\frac{(i - i_{dc})}{y_u}, \frac{K_{su}}{y_u\Lambda_u}\left(\frac{1}{2}y_u + h_c\right)\right]}_{\text{infiltration}} - \underbrace{\min\left(1.0, \frac{2\theta_u}{\varepsilon_u}\right)\frac{[e_p - \min(i, i_{dc})]}{y_u}}_{\text{transpiration}}$$
$$- \underbrace{\alpha_{us}\frac{K_u}{y_u^2}\left[\left(\frac{1}{2} - \frac{\theta_u}{\epsilon_u}\right)y_u + h_c\right]}_{\text{percolation/capillary rise}} + \underbrace{\frac{\theta_u}{y_u\omega_u}\frac{dy_s}{dt}}_{\text{water table change}} \tag{32}$$

$$\frac{dy_s}{dt} = \underbrace{\frac{\alpha_{us}K_u\omega_c}{\varepsilon_s y_u}\left[\left(\frac{1}{2} - \frac{\theta_u}{\varepsilon_u}\right)y_u + h_c\right]}_{\text{percolation/capillary rise}} - \underbrace{\frac{K_{ss}\omega_o}{\varepsilon_s\Lambda_s\cos\gamma_o}(h_s - h_o)}_{\text{groundwater exfiltration}} - \underbrace{\frac{K_{sr}l_rP_r}{A\varepsilon_s\Lambda_r}(h_s - h_r)}_{\text{base flow}}$$
$$- \underbrace{\frac{\alpha_{si}}{A\varepsilon_s}(h_s - h_{si})}_{\text{regional groundwater flow}} - \underbrace{\frac{G}{\varepsilon_s}}_{\text{sink/source}} \tag{33}$$

$$\frac{dm}{dt} = \underbrace{iw_r}_{\text{rainfall}} - \underbrace{e_pw_r}_{\text{evaporation}} + \underbrace{\frac{K_{sr}P_r}{\Lambda_r}(h_s - h_r)}_{\text{base flow}} + \underbrace{2y_o\frac{1}{n}(\sin\gamma_o)^{1/2}(y_o)^{2/3}}_{\text{lateral flow from sat. overland flow area}}$$
$$+ \underbrace{\sum_i \frac{1}{2l_r}m_i(v_r + v_{ri})}_{\text{channel inflow}} - \underbrace{\frac{1}{2l_r}m(v_r + v_{rj})}_{\text{channel outflow}} \tag{34}$$

These five equations, supplemented with geometric relations as well as flux closure relations, form the mathematical core of the REWASH model code. For the solution of this system of equations, an adaptive-step-size controlled Runge-Kutta algorithm presented by Press et al. (1992) has been adopted. This algorithm, using the Cash and Karp (1990) approach, limits the local truncation error at every time step to achieve a higher accuracy and robustness of the solution scheme.

2.2.4. Treatment of sub-grid variability of soil properties within a REW

Since Beven (1984) showed that there is decay in hydraulic conductivity with soil depth and Kirkby (1997) discussed the form of porosity decay, we have applied a division of the soil column to take into account the sub-grid variability of soil properties. In the real world, the variability of soil properties is one of the factors that induce quick subsurface storm flow. Within a REW, the soil column is divided into two layers. The average porosity and saturated hydraulic conductivity of the upper layer are larger than those of the lower layer. It should be pointed out that this division of the soil profile does not necessarily coincide with the boundary between the unsaturated and saturated zones as the consequence of varying water table depth. Therefore, the effective porosity of these two zones should be updated in time. Applying a depth-weighted averaging method, the effective porosity of both subsurface zones are given by:

$$\begin{cases} \varepsilon_u = \left[\varepsilon'_u d_{up} + \varepsilon'_s \left(y_u - d_{up}\right)\right] / y_u & (\text{if } y_u > d_{up}) \\ \varepsilon_u = \varepsilon'_u & (\text{if } y_u \leq d_{up}) \end{cases} \tag{35}$$

$$\begin{cases} \varepsilon_s = \left[\varepsilon'_u \left(d_{up} - y_u\right) + \varepsilon'_s \left(z_{surf} - z_r - d_{up}\right)\right] / \left(z_{surf} - z_r - d_{up}\right) & (\text{if } y_u < d_{up}) \\ \varepsilon_s = \varepsilon'_s & (\text{if } y_u \geq d_{up}) \end{cases} \tag{36}$$

where ε'_u [-] and ε'_s [-] are the soil porosity of the upper layer and the lower layer of the soil column, respectively; d_{up} [L] is the depth of the upper soil layer. By this parameterisation, in combination with the field capacity threshold, which controls when

percolation takes place, the time scales of the flow processes in the two subsurface domains can be better represented.

3. Model Application

3.1. Site description

The Geer River Basin has been selected for this study. It is a tributary of the Meuse River, located in Belgium (Fig. 3). The drainage area covers about 490 km^2. The basin is characterised by a deep groundwater system, which is delimited at the southern end by a ridge separating it from the Meuse River. The substrata are made up by several layers of chalk stone with low permeability. The groundwater aquifer of the basin consists of Cretaceous chalks with a thickness ranging from a few meters in the south to about 100 m in the north. The aquifer is underlain by a layer of Smectite, which can be regarded as an impervious bottom boundary. The unsaturated zone above the aquifer can be up to 40 m. The groundwater catchment does not correspond to the surface hydrological divide and extends beyond the catchment boundaries, thus water most likely flows across the northern topographical divide. Moreover, there is groundwater abstraction from wells and there are drainage galleries in the basin. Spatial data, a DEM with 30 m×30 m resolution, as well as four years (1 January 1993–31 December 1996) of daily rainfall, potential evaporation and discharges at the outlet are available.

3.2. Model calibration and sensitivity analysis

The basin has been discretised into a finite number of sub-watersheds, i.e. REWs, and the river network linking each REW has been generated using the modified TARDEM software (Tarboton, 1997). A 2nd order threshold on the Strahler river order system (Strahler, 1957) resulted in 73 REWs (see Fig. 4).

3.2.1. Parameter assignment and manual calibration

The parameters of the model consist of the interception threshold, surface roughness and channel friction factor, soil properties and hydraulic characteristics. All these parameters are effective values at REW-scale. Owing to the lack of spatially distributed information of these parameters as well as some of the geometric properties, such as the average total soil depth, the depth of the upper soil layer, and the river bed transition layer depth, we assume that they are uniformly distributed over the entire river basin. The initial state of the river basin is also assumed spatially uniform. As a result, the model functions as a lumped model. On the other hand, it decreases the model parameters to a more manageable number and reduces drastically the calibration task, making a quick evaluation of the model at the early development stage possible. For the derivation of initial estimates of the parameters, we made a realistic guess based on published values. Rainfall and potential evaporation data, measured at Bierset gauging station (Fig. 4), and discharge data, measured at the outlet of the Geer river from 1 January 1993 to 31 December 1994 have been used for model calibration. No data measured at interior flow gauges was available.

Knowing that water flows across the northern divide of the river basin, we imposed a flux boundary condition for those REWs bordering the northern divide (REW12, REW13, REW25, REW26, REW27, REW52, REW69 and REW73). With respect to groundwater abstractions, sink terms have been synthesised as monthly time series on the basis of available data and introduced to the saturated zone mass balance equation for each REW.

By applying a trial-and-error method, expert knowledge has been used to identify parameter values. During manual calibration, the most sensitive parameters have been recognised and physically meaningful ranges for those parameters determined. While visually inspecting the goodness of fit (comparison of the simulated hydrograph against the observed), objective measures such as the Nash-Sutcliffe efficiency (R^2_{NS}, Nash and Sutcliffe, 1970), the percentage bias (δ_P) have been used to evaluate the fit. The

definition of R^2_{NS} and δ_B are given as follows:

$$R^2_{NS} = 1.0 - \frac{\sum_{i=1}^{n} (Q_{si} - Q_{oi})^2}{\sum_{i=1}^{n} (Q_{oi} - \bar{Q}_o)^2} \tag{37}$$

where Q_{si}, Q_{oi} and $\bar{Q}_o$ are the simulated discharge, the observed discharge at the time step i and the mean of the observed discharge respectively.

$$\delta_B = \left| \frac{\sum_{i=1}^{n} (Q_{si} - Q_{oi})}{\sum_{i=1}^{n} Q_{oi}} \right| \times 100\% \tag{38}$$

where δ_B represents the difference of the total volume between the simulated and observed time series. The bias is an important measure to evaluate simulations of continuous models.

3.2.2. Sensitivity analysis

Sensitivity analysis is a useful tool to assess the effect of parameter perturbations on model output. Starting with the manual calibration, each parameter has been varied by +50% and −50% while the other parameters were maintained unchanged. Having gained a knowledge of which parameters are most sensitive in manual calibration, we chose six parameters (i_{dc}, K_{su}, K_{ss}, ε'_s, ε'_u, λ) to further evaluate model sensitivity. Using the relative change in runoff volume (δ_V) and the relative change in Nash-Sutcliffe efficiency (δ_{NS}) as indices, the effect of each parameter change on the runoff-producing events during the period from 1 January 1993 to 31 December 1993 has been anal-

ysed. δ_V and δ_{NS} are defined as follows:

$$\delta_V = \left| \frac{\sum_{i=1}^{n} (Q_{i+} - Q_{i-})}{\sum_{i=1}^{n} Q_{im}} \right| \times 100\% \tag{39}$$

where Q_{i+}, Q_{i-} and Q_{im} refer to the discharges at the time step i with the parameter value varied by +50%, −50% and the manually calibrated parameter value, respectively. The larger the δ_V, the more sensitive the model is to the parameter under study.

$$\delta_{NS} = \left| \frac{R^2_{NS+} - R^2_{NS-}}{R^2_{NSm}} \right| \times 100\% \tag{40}$$

where R^2_{NS+}, R^2_{NS-} and R^2_{NSm} are the Nash-Sutcliffe efficiency values with the parameter value varied by +50%, −50% and the manually calibrated parameter value, respectively. Same as δ_V, the larger the δ_{NS}, the more sensitive the model to the parameter under study.

3.2.3. Automated parameter optimisation

A hybrid approach combining manual and automated calibration methods is increasingly recognised as a more efficient way of parameter optimisation (Douglas et al., 2000). Following the trial-and-error procedure, we carried out an automatic calibration procedure to enhance the accuracy of the model optimisation. During the manual calibration, physically reasonable ranges of parameter values have been delineated. These ranges were then prescribed in the automatic calibration procedure for the fine adjustment of parameter values. In this work, the optimisation tool GLOBE (Solomatine, 1995, 1998) has been coupled to REWASH. Figure 5 shows the loop of the automated calibration procedure. P_obj and P_update are the two programmes linking REWASH to GLOBE. These programmes are driven by GLOBE in each evaluation

loop, in which P_update takes the values of the parameter set generated from GLOBE and updates the input files for the REWASH, and P_obj provides the error value calculated with a specified objective function (i.e. R^2_{NS} for this work) to GLOBE.

3.3. Model verification

Model verification has been carried out to test whether the model, using the same parameter set obtained by optimisation, but with independent data sets, can produce outputs with reasonable accuracy. A classical method for model verification, the split-sample test (Klemeš, 1986) has been applied since there is no indication that there has been an abrupt change of the basin characteristics and conditions over the time domain of the investigation. The data set from 1 January 1995 to 31 December 1996 has been used for the verification test. To examine whether the model can perform in a consistent manner in terms of simulating the real system within the range of accuracy, a model validity test has been conducted by reversing calibration and verification periods. In this analysis, the data set of the period from 1 January 1995 to 31 December 1996 is used for calibration while the other part of the data set is for verification.

4. Results and discussion

4.1. Model calibration

After manual and automatic calibration with a limited number of parameters (i_{dc}, K_{su}, K_{ss}, ε'_s, ε'_u, λ), the Nash-Sutcliffe efficiency of the model reached 0.71, while the volume error represented by δ_B was only 0.76%. Table 1 lists the accepted best parameter values and the model performance. The values of the saturated hydraulic conductivity of the unsaturated zone and the soil porosity of the upper soil layer are more than twice as high as those of the saturated zone and of the lower soil layer, respectively. The λ value indicates that the soil type is silty loam, which agrees with other soil property indicators, such as K_{su} and ε'_u.

Figure 6 shows the comparison of the simulated and observed hydrographs (Fig. 6b), and the accumulated discharges for the simulated and observed data at the outlet of the Geer river basin (Fig. 6c). Clearly, the watershed response to the atmospheric forcing is well captured. The base flow is quite accurately reproduced in the calibration period except for the beginning 3 months, mostly due to the model warming up effect. Most peaks are simulated with reasonable accuracy although some peaks in the period from 340 days to 480 days (Fig. 6b) are underestimated. We also observed that three peaks in the period from 560 days to 580 days are overestimated compared with the measured data. However, we argue that these under- and overestimation for the peaks are not entirely due to the modelling errors but also subject to data errors and the spatial distribution of rainfall. If we examine the rainfall data (Fig. 6a) in the period between day 560 and day 580, there are three rainfall events with relatively high rainfall intensity ranging from 11.8 to 24.4 mm/d. These events should have produced higher stream flows than observed. The inconsistency between the rainfall observations and the discharge measurements is mostly due to the fact that only one rainfall station was used for the simulation. Figure 7 shows the flow duration curves for the simulated and observed discharges. It also confirms that low flows are better simulated than middle-ranged flows when comparing to measured data. Yet we realise that the model involves parameter uncertainties since there are no catchment-scale parameters ever measured or detailed data on state variables other than discharge to confirm the calibrated model parameters. This remains a challenge for ongoing and future research, especially since field measurement technique do not measure catchment-scale variables and parameters.

4.2. Model sensitivity to parameters

A set of computer runs has been implemented to test model sensitivity to parameters listed in Table 2. The analysis primarily focused on subsurface parameters. Table 2 shows that runoff simulations are most sensitive to the soil pore-disconnectedness λ and the soil porosity of the lower soil layer ε'_s. λ mostly affects the runoff volume while

ε'_s has the strongest effect on the Nash-Sutcliffe efficiency. This can be explained if we recall the equations described in Sect. 2. From Eq. (10), (14), (15) and (32), we see that λ is the one that determines the unsaturated hydraulic conductivity and the unsaturated zone hydraulic potential, and hence the infiltration capacity and the percolation flux. From Eq. (33), one can observe that ε'_sdictates the subsurface storage and interactions between surface and subsurface flows. Meanwhile, these equations also explain the significance of K_{ss} and ε'_uin model performance. The test results already suggested a remarkable effect of the interception threshold i_{dc} on runoff generation although it's sensitivity is smaller than the subsurface parameters. The effect of i_{dc} is discussed in more details in the following section.

4.3. Effect of interception

Applying the same forcing input, identical initial and boundary conditions, and the same parameters tuned in the model including interception (Fig. 6), the model excluding interception has been re-calibrated automatically. Figure 8 shows the comparison of the simulated hydrograph and the observed. Apparently, the model without interception performed much worse than the one with interception: R^2_{NS} is 14% lower, and δ_B is 187% larger. Figure 9 shows the flow duration curves for the simulation outputs of both the models with and without interception, as well as for the observed flow records. It clearly shows that the model without interception does not cover the full range of the low flows, suggesting erroneous simulation of the water balance. This is because more water, which would have been intercepted, is adding to the subsurface stores, participating in the surface and subsurface flux exchanges, and subsequently contributes to stream flow. Especially during the smaller rainfall events, the part of the rainfall flux that would have been intercepted leads to a higher antecedent soil moisture state, which either initiates a quicker surface runoff or gives rise to higher stream flow during the low flow regime. In the simulation without interception, we see that low flows are higher than observed, e.g. in the period of the last 120 days (Fig. 8a). However, as the model tries to maintain overall performance in terms of total volume, the simulated flow mass

curve enters into a more or less constant slope, which does not follow the bending of the observed flow mass curve after 360 days (Fig. 8b). In Fig. 10, one can notice that without interception, the soil saturation is steadily increasing over time (dotted lines) for each of the REWs presented. However, one would expect that for a multiple-year simulation, the soil moisture state would preserve an equilibrium state while varying seasonally.

4.4. Model verification

The approach suggested by Kleměs (1986) has been adopted to verify the model. A reversed calibration/verification test was also carried out. From Fig. 11, we can see that the model is able to reproduce most peaks except the one on day 525. The observed discharge on this day is 9 m^3/s and the rainfall causing this peak is 28 mm/d. Scanning all rainfall events and peak responses in the catchment in the period of 1993–1996, this data point is an outlier, which can not be used for model performance analysis. In this verification run, low flows in most of the time are underestimated, which can be confirmed from the flow duration curve (Fig. 12). Actually, from Fig. 11b), we can find that the observed flow data exhibit more or less constant base flows and show no remarkable depleting trend in the dry period over the time from 1995 to 1996. This appearance is also shown in Fig. 12 in which there is an abrupt change of the probability distribution for the observed discharges from 2.0 m^3/s to 1.0 m^3/s.

Table 3 reports the summary of the model performance in each of the calibration/verification runs. Figure 13 and Fig. 14 present the reversed calibration/verification tests. All these results demonstrate that the model, giving a similar volume error and Nash-Sutcliffe efficiency in each of the simulations, performs in a very consistent manner.

5. Summary and conclusions

This is the first time that the REW approach has been applied to a real-world situation with convincing results. A numerical model has been constructed, and enhanced by the addition of the interception process, improved transpiration scheme and improved saturation-excess flow area formulation. At the watershed-scale, surface and subsurface interaction, climate feedback, hill-slope and channel network have been fully coupled, based on physical principles. To enhance the model's numerical efficiency and stability, the momentum balance equations have been simplified by ignoring inertia terms, leading to algebraic forms of exchange fluxes. The mass balance equations have been converted into univariate derivative form so that a single variable is computed to represent the state of each flow domain at each time step. An adaptive-step-size controlled Runge-Kutta integration algorithm has been applied to solve the coupled system of equations, ensuring model stability while maintaining accuracy. The model has been coupled to the GLOBE optimization tool for automatic calibration.

The model has been applied to the Geer river basin, which lies in a temperate humid climate region. This basin has a complex subsurface where the natural groundwater basin does not coincide with the surface water divide. It is further complicated by human interference through pumping and artificial underground drainage, giving rise to a great deal of difficulty in modelling its hydrological response.

Model calibration was carried out using a combined manual and automatic method. The sample-split test resulted in a similar accuracy, suggesting that the model performs in a consistent manner in the study area. Judging by the Nash-Sutcliffe efficiency and volume percentage bias, it can be concluded that the simulated stream flows are reasonably accurate.

The introduction of interception in the model, in spite of the simplicity of the approach, showed that it improved the soil moisture accounting, resulting in a better stream flow simulation. Subject to the research objective, a more sophisticated module for interception, taking into account the effect of temporal and spatial variation due to vegetation

type and their seasonal changes can be further investigated in the future.

This paper demonstrates that the model presented here is capable of capturing watershed responses and simulating rainfall-runoff behaviour. Although there is still substantial work to be done before the model can be routinely applied in catchments with different physio-geographic and climatic settings, the model presented here provides a general modelling framework as an alternative for physically based distributed modelling. One can tune this model or modify any functional relation to suite the characteristics of a specific study site.

Appendix A: Nomenclature

Dimensions: L, length; T, time; M, mass.

A	horizontally projected surface area of a REW [L^2].
d_{up}	depth of the upper soil layer [L].
e_p	potential evaporation [LT^{-1}].
e_{ctop},e_{otop},e_{rtop}	rainfall flux to Czone, to Ozone and to River [L^3T^{-1}].
e_{ca}, e_{cu}, e_{co}	interception flux from Czone, infiltration flux to Uzone, flux between Czone and Ozone [L^3T^{-1}].
e_{oa}, e_{os}, e_{or}, e_{oc}	evaporation flux from Ozone, flux between Ozone and Szone, flux between Ozone and River, flux between Ozone and Czone [L^3T^{-1}].
e_{ua}, e_{uc}, e_{us}	transpiration flux in Uzone, infiltration flux from Czone, percolation/ capillary rise flux [L^3T^{-1}].
e_{su}, e_{so}	the counterpart of e_{us} and e_{so}.
e_{sr}, e_{si}, e_{sa}	flux between Szone and River, flux exchange between the neighbouring REWs, groundwater abstraction [L^3T^{-1}].
e_{ra}, e_{rin}, e_{rout}	evaporation from River, flux from upstream River, flux to the downstream River [L^3T^{-1}].
e_{rs}, e_{ro}	the counterpart of e_{sr} and e_{or}.
f	infiltration capacity [L^3T^{-1}].
g	gravitational acceleration [LT^{-2}].
G	groundwater abstraction or recharge rate [L^3T^{-1}].
h_c	capillary pressure head [L].
h_o, h_r, h_s	total hydraulic head for Ozone, River and Szone [L].
i	precipitation intensity [LT^{-1}].
i_{dc}	interception threshold for Czone [LT^{-1}].
K_{su}, K_u	saturated and effective hydraulic conductivity for Uzone [LT^{-1}].
K_{sr},K_{ss}	saturated hydraulic conductivity for riverbed and Szone[LT^{-1}].

l_r	length of the river channel [L].
m	average cross-sectional area [L^2].
n	Manning roughness coefficient [$TL^{1/3}$].
P_r	wetted perimeter of the river cross section [L].
Q_{si}, Q_{oi},$\bar{Q}_o$	simulated discharge, observed discharge at the time step i, mean of the observed discharge [L^3T^{-1}].
Q_{i+}, Q_{i-}, Q_{im}	discharges after the parameter perturbation by ±50% at time step i, discharge after the accepted manual calibration at time step i [L^3T^{-1}].
R^2_{NS}	Nash-Sutcliffe efficiency [-].
R^2_{NS+}, R^2_{NS-}, R^2_{NSm}	R^2_{NS} values after parameter perturbation by ±50%, and after the accepted manual calibration [-].
s	sink or source term.
S_c, S_o, S_u, S_s, S_r	storage of Czone, Ozone, Uzone, Szone and River [L^3].
v_o, v_r	velocity of the flow in the River and Ozone [LT^{-1}].
w_r	width of the river channel [L].
y_o	depth of flow sheet over the overland flow zone surface [L].
y_r	water depth of the river channel [L].
y_s, y_u	average depth of Szone and Uzone[L].
z_r, z_s, z_{surf}	average elevation for river bed, ground surface and soil bottom [L].
Z	average soil depth [L].
α_{sf}	scaling factor for Ozone area computation [-].
α_{si}	lumped scaling factor for regional groundwater flow [L^2T^{-1}].
α_{us}	scaling factor for flux exchange between Uzone and Szone [-].
δ_B	discharge volume percentage bias [-].
δ_{NS}	relative change in Nash-Sutcliffe efficiency [-].
δ_V	relative change in percentage bias [-].
ε'_u, ε'_s	porosity of the upper and lower soil layer [-].

ε_u, ε_s	effective soil porosity of Uzone and Szone [-].
ϕ	generic thermodynamic property.
γ_o	average surface slope angle of Ozone in radian.
γ_r	average slope angle of the channel bed in radian.
λ	soil pore-disconnectedness index [-].
Λ_r	depth of the transition zone of the river bed for the base flow [L].
Λ_s	typical length scale for the exfiltration flux (seepage) [L].
Λ_u	length scale of the wetting front for infiltration [L].
μ	soil pore size distribution index [-].
θ_f	field capacity of Uzone [-].
ρ	water density [ML^{-3}].
ω_o, ω_c, ω_o,	area fraction of the saturation-excess overland flow domain, infiltration-excess flow domain and the unsaturated flow domain [-].
ξ	Darcy-Weisbach friction factor for the channel routing [-].
ψ_b	air entry pressure head at Uzone [L].

Acknowledgements. This research has been funded by Delft Cluster project Oppervlaktewater hydrologie: 06.03.04. We are very grateful to D. P. Solomatine of UNESCO-IHE for providing the GLOBE optimisation software for automatic calibration. We acknowledge that the data applied in this research were acquired through the project DAUFIN, sponsored by the European Commission within FP5: EVK1-CT1999-00022. The Hydrogeology team of the University of Liège (Belgium) and especially S. Brouyère and A. Dassargues provided the basic data about the geological and hydrogeological conditions in the Geer basin. The Royal Meteorological Observatory (KMI) in Brussels and E. Roulin provided the digital elevation maps and the hydrometeorological data.

References

Abbott, M. B., Bathurst, J. C., Cunge, J. A., O'Connell, P. E., and Rasmussen, J.: An introduction to the European Hydrologic System Systeme Hydrologique Europeen, SHE, 1: History

and philosophy of a physically based, distributed modelling system, J. Hydrol., 87, 45–59, 1986a.
Abbott, M. B., Bathurst, J. C., Cunge, J. A., O'Connell, P. E., and Rasmussen, J.: An introduction to the European Hydrologic System Systeme Hydrologique Europeen, SHE, 2: Structure of a physically based, distributed modelling system, J. Hydrol., 87, 61–77, 1986b.
Bergström, S. and Forsman, A.: Development of a conceptual deterministic rainfall-runoff model, Nordic Hydrol., 4, 147–170, 1973.
Bergström, S.: The HBV model, in: Computer models of watershed hydrology, edited by: Singh, V. P., Water Resources Publications, USA, pp. 443–520, 1995.
Beven, K. J.: Infiltration into a class of vertically non-uniform soils, Hydrol. Sci. J., 29, 425–434, 1984.
Beven, K. J.: Changing ideas in hydrology: the case of physically based models, J. Hydrol., 105, 157–172, 1989.
Beven, K. J.: Prophesy, reality and uncertainty in distributed hydrological modelling, Adv. Water Res., 16, 41–51, 1993.
Beven, K. J.: A discussion of distributed hydrological modelling, in: Distributed hydrological modelling, edited by: Abbott, M. B. and Refsgaard, J. C., Kluwer Academic Publishers, Dordrecht, The Netherlands, pp. 255–278, 1996a.
Beven, K. J.: Response to comments on "A discussion of distributed hydrological modelling" by J. C. Refsgaard et al., in: Distributed hydrological modelling, edited by: Abbott, M. B. and Refsgaard, J. C., Kluwer Academic Publishers, Dordrecht, The Netherlands, pp. 289–295, 1996b.
Beven, K. J.: Equifinality and uncertainty in geomorphological modelling, in: The scientific nature of geomorphology, edited by: Rhoads, B. L. and Thorn, C. E., John Wily & Sons, Chichester, UK, pp. 289–313, 1996c.
Beven, K. J.: Towards an alternative blueprint for a physically based digitally simulated hydrologic response modelling system, Hydrol. Process., 16, 189–206, 2002.
Beven, K. J., Calver, A., and Morris, E.: The Institute of Hydrology distributed model, Institute of Hydrology Report No. 98, UK, 1987.
Beven, K. J., Lamb, R., Quinn, P., Romanowicz, R., and Freer, J.: TOPMODEL, in: Computer models of watershed hydrology, edited by: Singh, V. P., Water Resources Publications, USA, pp. 627–668, 1995.
Blöschl, G. and Sivapalan, M.: Scale issues in hydrological modelling – a review, Hydrol. Pro-

cess., 9, 251–290, 1995.
Brooks, R. H. and Corey, A. T.: Hydraulic properties of porous media, Hydrol. Pap. No. 3, Colorado State Univ., Fort Collins, 1964.
Burnash, R. J. C., Ferral, R. L., and McGuire, R. A.: A Generalized streamflow simulation system – Conceptual modeling for digital computers, U.S. Department of Commerce, National Weather Service and State of Califonia, Department of Water Resources, 1973.
Burnash, R. J. C.: The NWS river forecast system – Catchment modelling, in: Computer models of watershed hydrology, edited by: Singh, V. P., Water Resources Publications, USA, pp. 311–366, 1995.
Calver, A. and Wood, W. L.: The Institute of Hydrology distributed model, in: Computer models of watershed hydrology, edited by: Singh, V. P., Water Resources Publications, USA, pp. 595–626, 1995.
Cash, J. R. and Karp, A. H.: ACM Transactions on Mathematical Software, 16, 201–222, 1990.
Douglas, P. B., Gupta, H. V., and Sorooshian, S.: Toward improved calibration of hydrologic models: Combining the strengths of manual and automatic methods, Water Resour. Res., 36, 3663–3674, 2000.
Dunne, T. and Black, R. D.: Partial area contributions to storm runoff in a small New England watershed, Water Resour. Res., 6, 1296–1311, 1970.
Dunne, T.: Field studies of hillslope flow processes, in: Hillslope Hydrology, edited by: Kirkby, M. J., John Wily & Sons, Chichester, UK, pp. 227–293, 1978.
Freeze, R. A. and Harlan, R. L.: Blueprint for a physically-based, digitally-simulated hydrologic response model, J. Hydrol., 9, 237–258, 1969.
Grayson, R. B., Moore, I. D., and McMahon, T. A.: Physically based hydrologic modeling, 1, A terrain-based model for investigative purposes, Water Resour. Res., 28, 2639–2658, 1992.
Grayson, R. B., Moore, I. D., and McMahon, T. A.: Physically based hydrologic modeling, 2, Is the concept realistic?, Water Resour. Res., 28, 2659–2666, 1992.
Hewlett, J. D. and Hibbert, A. R.: Factors affecting the response of small watersheds to precipitation in humid areas, in: Proceedings of 1st International Symposium on Forest Hydrology, edited by: Sopper, W. E. and Lull, H. W., Pergamon, pp. 275–290, 1967.
Kirkby, M. J.: TOPMODEL: A personal view, Hydol. Process., 11, 1087–1097, 1997.
Klemeš, V.: Operational testing of hydrological simulation models, Hydrol. Sci. J., 31, 13–24, 1986.
Lindström, G., Johansson, B., Persson, M., Gardelin, M., and Bergström, S.: Development and

test of the distributed HBV-96 hydrological model, J. Hydrol., 201, 272–288, 1997.
Nash, J. E. and Sutcliffe, J. V.: River flow forecasting through conceptual models, Part I: a discussion of principles, J. Hydrol., 10, 282–290, 1970.
O'Connell, P. E. and Todini, E.: Modelling of rainfall, flow and mass transport in hydrological systems: an overview, J. Hydrol., 175, 3–16, 1996.
Press, W. H., Teukolsky, S. A., Vetterling, W. T., and Flannery, B. P.: Numerical recipes in C: The art of scientific computing, 2nd Edition, Cambridge University Press, pp. 710–722, 1992.
Refsgaard, J. C. and Storm, B.: MIKE SHE, in: Computer models of watershed hydrology, edited by: Singh, V. P., Water Resources Publications, USA, pp. 809–846, 1995.
Refsgaard, J. C., Storm, B., and Abbott, M. B.: Comment on "A discussion of distributed hydrological modelling" by K. Beven, in: Distributed hydrological modelling, edited by: Abbott, M. B. and Refsgaard, J. C., Kluwer Academic Publishers, Dordrecht, The Netherlands, pp. 279–287, 1996.
Reggiani, P. and Schellekens, J.: Modelling of hydrological responses: the representative elementary watershed approach as an alternative blueprint for watershed modelling, Hydrol. Process., 17, 3785–3789, 2003.
Reggiani, P., Sivapalan M., and Hassanizadeh, S. M.: A unifying framework of watershed thermodynamics: balance equations for mass, momentum, energy and entropy and the second law of thermodynamics, Adv. Water Res., 22, 367–368, 1998.
Reggiani, P., Sivapalan, M., and Hassanizadeh, S. M.: Conservation equations governing hillslope responses: Physical basis of water balance, Water Resour. Res., 38, 1845–1863, 2000.
Reggiani, P., Hassanizadeh, S. M., Sivapalan, M., and Gray, W. G.: A unifying framework of watershed thermodynamics: Constitutive relationships, Adv. Water Res., 23, 15–39, 1999.
Reggiani, P., Sivapalan, M., Hassanizadeh, S. M., and Gray, W. G.: Coupled equations for mass and momentum balance in a stream network: theoretical derivation and computational experiments, Proc. R. Soc. Lond. A (2001), 457, 157–189, 2001.
Reggiani, P. and Rientjes, T. H. M.: Flux parameterization in the Representative Elementary Watershed (REW) Approach: application to a natural basin, Water Resour. Res., W04013(1-8), 2005.
Savenije, H. H. G.: Equifiniality, a blessing in disguise?, Hydrol. Process., 15, 2835–2838, 2001.
Savenije, H. H. G.: The importance of interception and why we should delete the term evapo-

transpiration from our vocabulary, Hydrol. Process., 18, 1507–1511, 2004.
Savenije, H. H. G.: Interception, The Encyclopaedia of Water, Wiley, 2005.
Sivapalan, M., Viney, N. R., and Jeevaraj, C. G.: Water and salt balance modelling to predict the effects of land use changes in forested catchments: 3. The large catchment model, Hydrolog. Process., 10, 429–446, 1996.
Solomatine, D. P.: Genetic and other global optimization algorithms – comparison and use in calibration problems, in: Proceedings of the 3rd International Conference on Hydroinformatics, Copenhagen, Denmark, Balkema Publishers, pp. 1021–1028, 1998.
Solomatine, D. P.: The use of global random search methods for models calibration, in: Proceedings of XXVIth Congress of the International Association for Hydraulic Research (IAHR), vol. 1, London, pp. 224–229, 1995.
Strahler, A. N.: Quantitative analysis of watershed geomorphology, American Geophysical Union Transactions, 38, 913–920, 1957.
Tarboton, D. G.: A new method for the determination of flow directions and contributing areas in grid digital elevation models, Water Resour. Res., 33, 309–319, 1997.
Todini, E.: The ARNO rainfall-runoff model, J. Hydrol., 175, 339–382, 1996.
Zhang, G., Reggiani, P., Rientjes, T. H. M., and Hassanizadeh, S. M.: Modeling rainfall-runoff relation by the Representative Elementary Watershed Approach, in: Proceedings of NCR-days 2002: Current themes in Dutch river research, edited by: Leuven, R. S. E. W., van Os, A. G., and Nienhuis, P. H., NCR-publication 20-2003, Netherlands Centre for River Studies, Delft, The Netherlands, pp. 20–22, 2003.
Zhang, G. P., Fenicia, F., Rientjes, T. H. M., Reggiani, P., and Savenije, H. H. G.: Effects of subsurface parameterisation on runoff generation in the Geer basin, in: Proceedings of NCR-days 2003: Dealing with Floods within Constraints, edited by: Douben, N. and van Os, A. G., NCR publication 24-2004, Netherlands Centre for River Studies, Delft, The Netherlands, pp. 68–70, 2004a.
Zhang, G. P., Fenicia, F., Rientjes, T. H. M., Reggiani, P., and Savenije, H. H. G.: Application and development of a catchment-scale rainfall-runoff model using the REW approach, Geophys. Res. Abstr., 6, 01583, European Geosciences Union, 2004b.
Zhang, G. P., Fenicia, F., Rientjes, T. H. M., Reggiani, P., and Savenije, H. H. G.: Modeling runoff generation in the Geer River Basin with improved model parameterizations to the REW approach, Phys. Chem. Earth, in press, 2005a.
Zhang, G. P., Savenije, H. H. G., Fenicia, F., Rientjes, T. H. M., and Reggiani, P.: Implications

of hydrological modelling and observations in the Alzette river basin, in: Proceedings of NCR-days 2004: Research for managing rivers; present and future issues, in press, 2005b.

Table 1. The accepted best parameter values for the calibration period and the model performance.

Parameters	i_{dc} [mm/d]	n [s/m$^{1/3}$]	K_{ss} [m/d]	K_{su} [m/d]	K_{sr} [m/d]	ε'_s [-]	ε'_u [-]	λ [-]	θ_f [-]
Value	1.36	0.020	0.0097	0.0213	2.64	0.148	0.43	4.43	0.08
R^2_{NSE}	0.71								
δ_{PB}	0.76%								

Table 2. Sensitivity of the model output to parameters.

Parameters	δ_V(%)	δ_{NS} (%)
λ [-]	190	1177
ε'_s [-]	109	1729
K_{ss} [m/d]	81	45
ε'_u [-]	77	89
K_{su} [m/d]	10	6
i_{dc} [mm/d]	10	5

Table 3. Model performance in the split-sample test runs.

test	δ_B(%)	R^2_{NS}
calibration (1993–1994)	0.76	0.71
verification (1995–1996)	4.79	0.61
reversed calibration (1995–1996)	4.14	0.65
reversed verification (1993–1994)	3.82	0.68

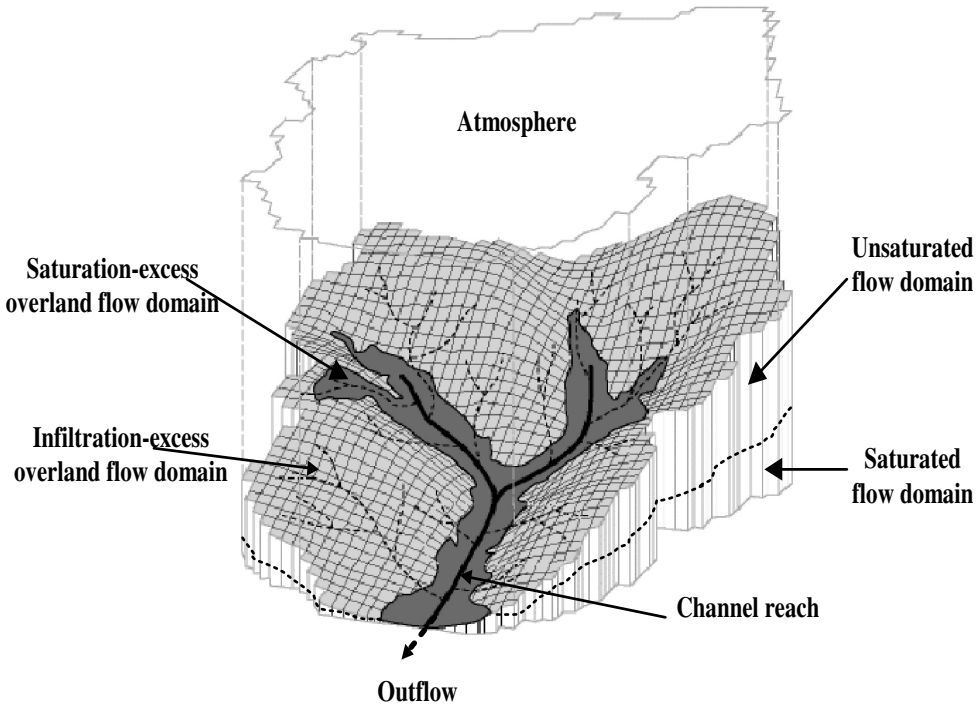

Fig. 1. A 3-D view of the volume comprising a single REW (modified from Reggiani and Schellekens, 2003).

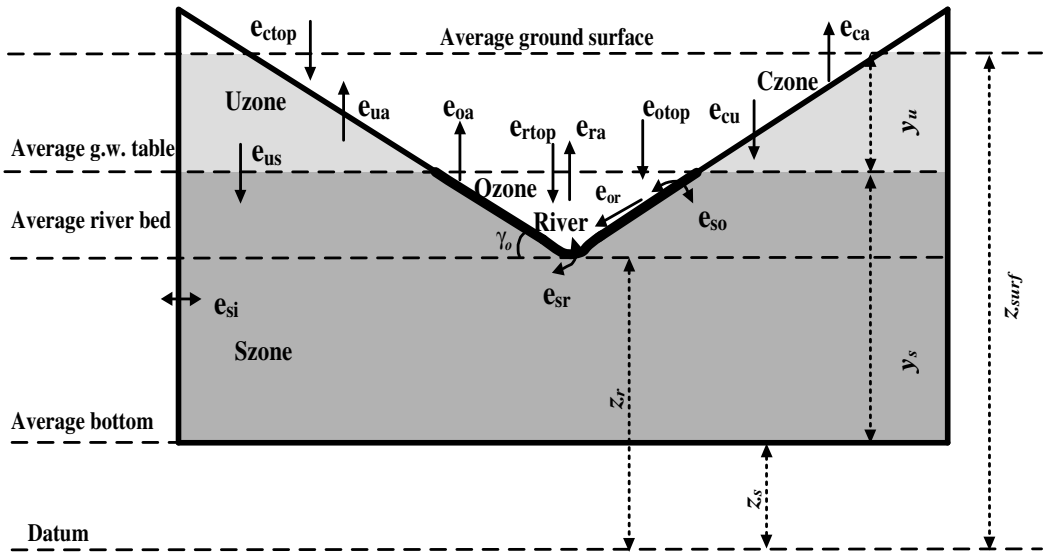

Fig. 2. Schematised cross-sectional profile of a REW. Czone, Ozone, Uzone, Szone and River stand for the infiltration-excess overland flow domain, the saturation-excess overland flow domain, the unsaturated flow domain, the saturated flow domain and the River flow domain, respectively. e_{ctop}, e_{cu}, e_{ca} etc. are flux terms. y_u, y_s are stock variables, and z_s, z_r, z_{surf} and γ_o are average geometric quantities of the REW.

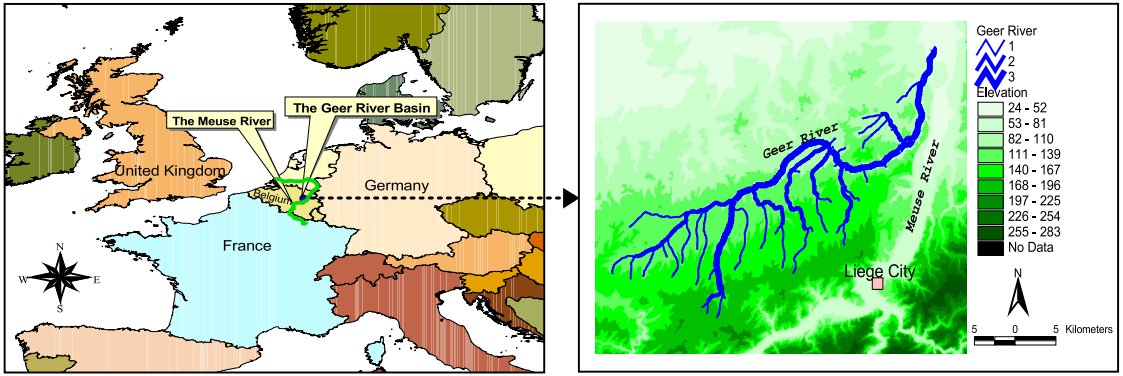

Fig. 3. Location of the Geer river basin and the Geer river network.

HESSD
2, 639–690, 2005

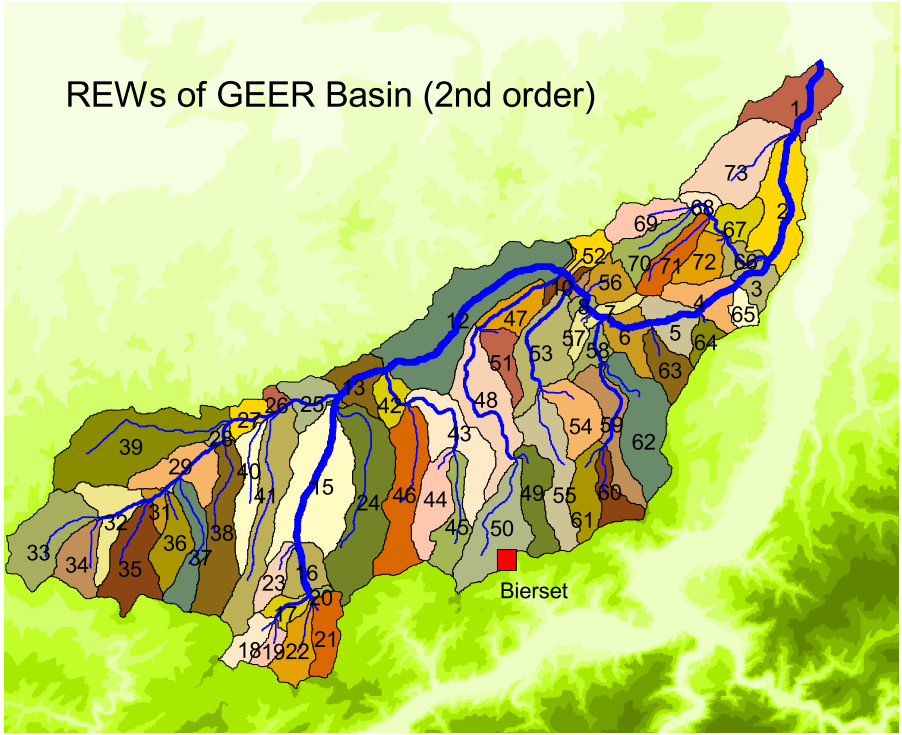

Fig. 4. Discretisation of the Geer river basin and the resultant REWs.

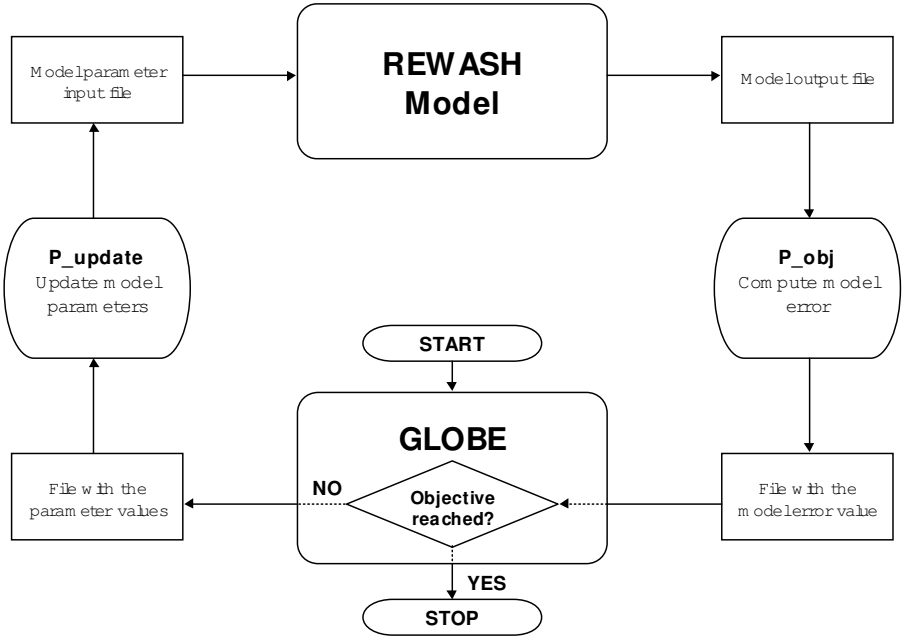

Fig. 5. Flow chart of the automatic calibration procedure (after Solomatine, 1998).

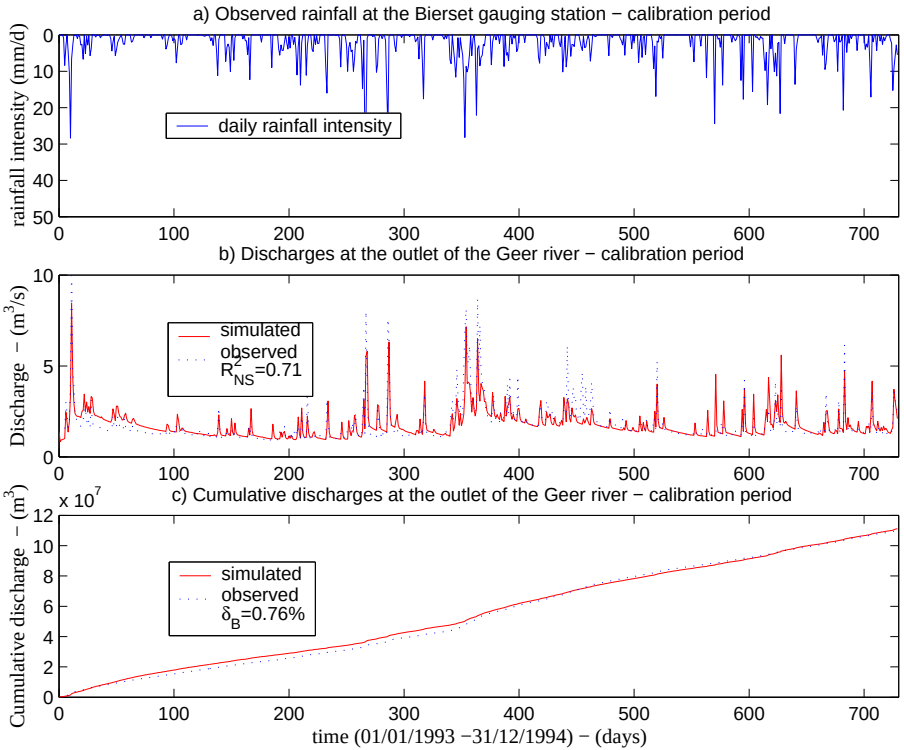

Fig. 6. Comparison of the simulated and the observed hydrograph and cumulative discharge volume at the basin outlet for the calibration period (1 January 1993–31 December 1994): **(a)** the rainfall, **(b)** the observed and simulated discharge, **(c)** the accumulated observed and simulated runoff.

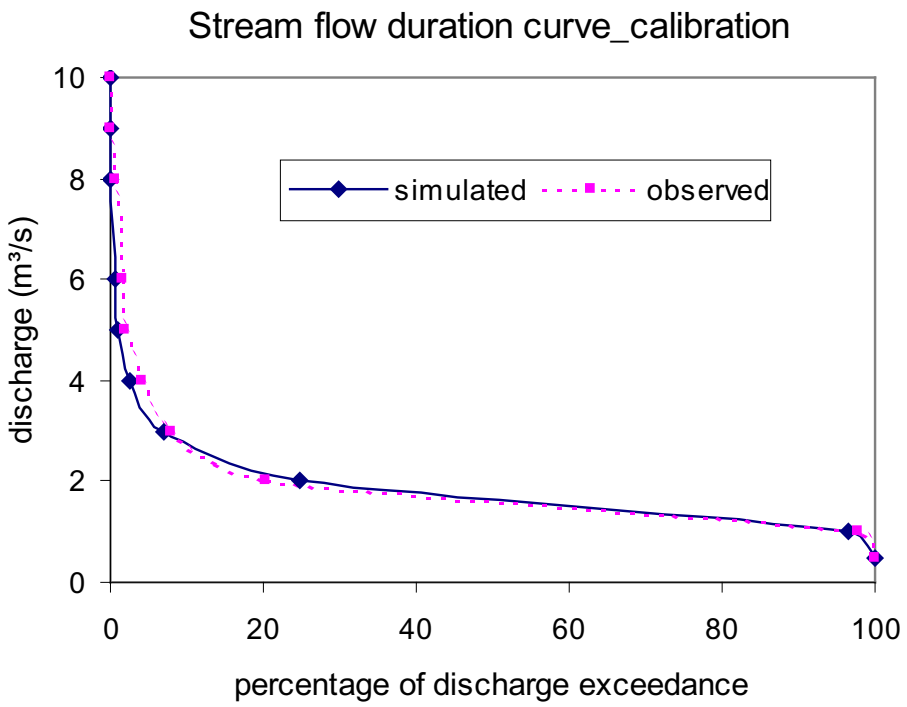

Fig. 7. Flow duration curves for the model calibration results and the observed data.

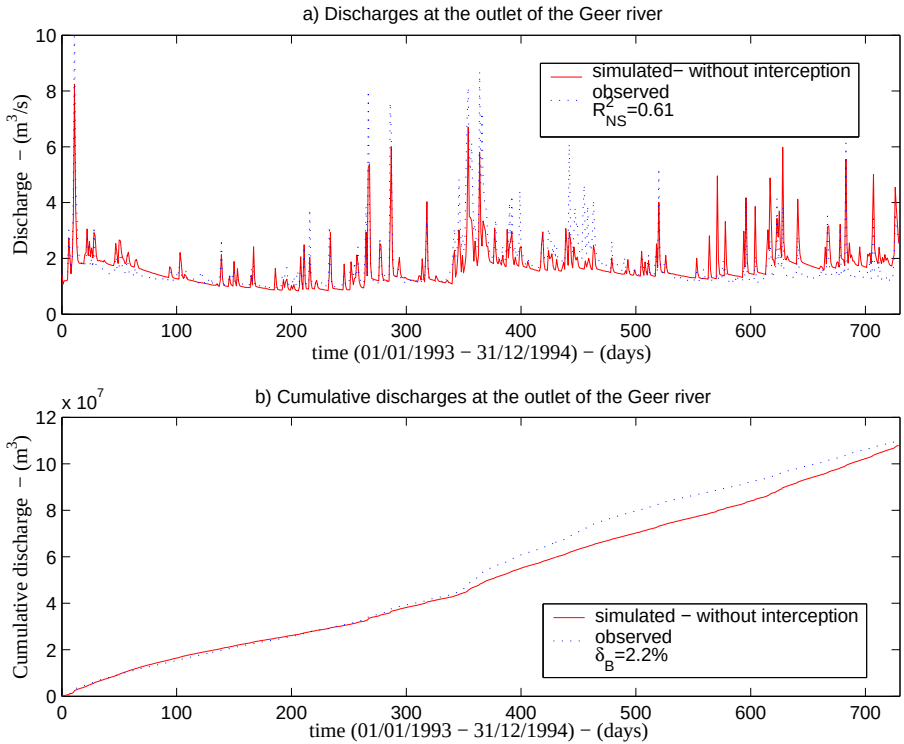

Fig. 8. Simulated discharge using the model without interception after optimisation (1 January 1993–31 December 1994): **(a)** observed and simulated discharge, **(b)** accumulated observed and simulated runoff.

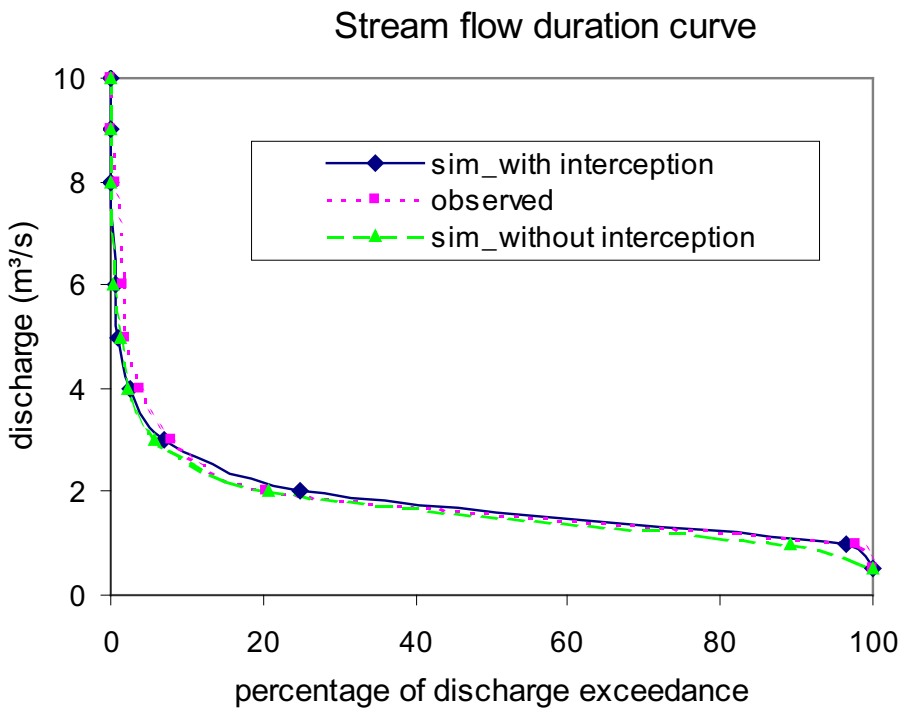

Fig. 9. Flow duration curves for the model calibration results (with interception and without interception) and the observed data.

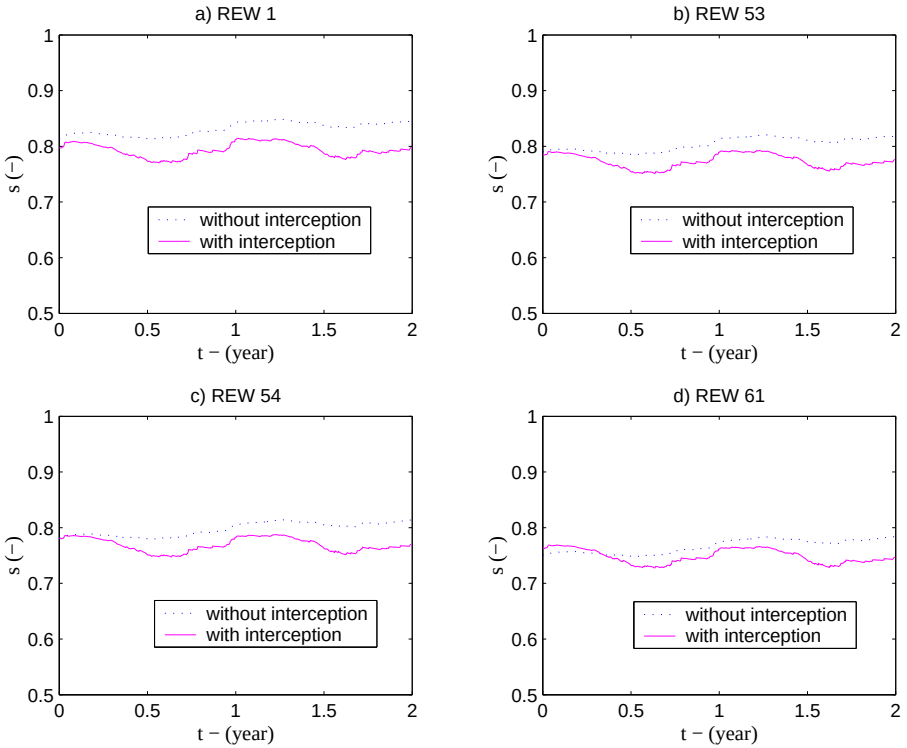

Fig. 10. Comparison of the hill-slope soil moisture dynamics simulated with and without interception process in the model. REW 53, REW 54 and REW 61 compose a hill-slope of the catchment in the southern side of the Geer river.

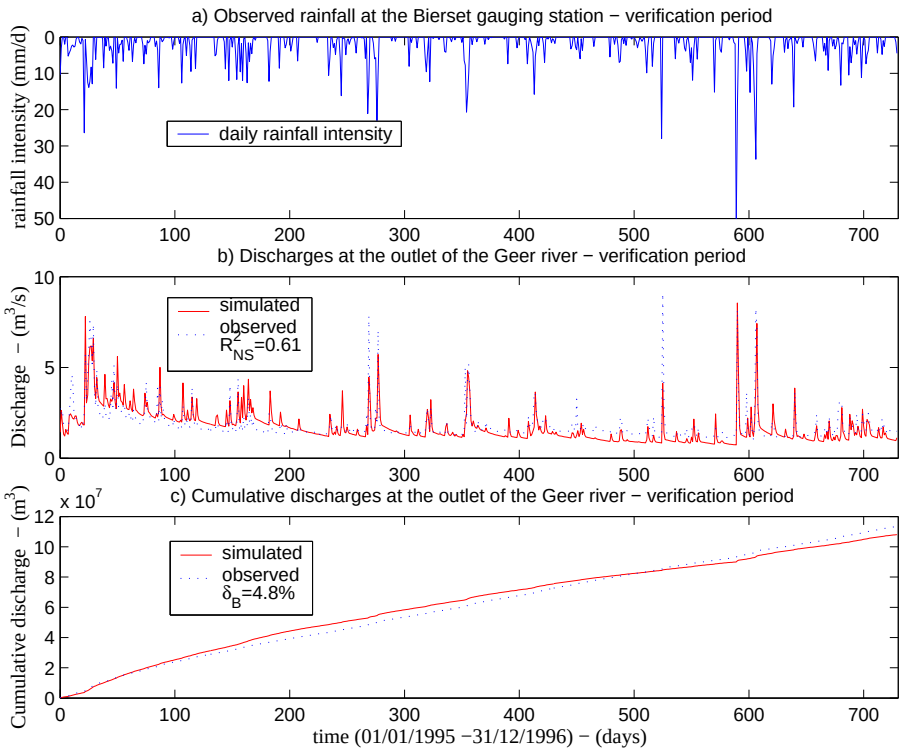

Fig. 11. Model verification results: **(a)** observed daily rainfall intensity at the Bierset station; **(b)** comparison of the simulated and observed daily discharge at the outlet of the Geer river basin; **(c)** comparison of the simulated and observed runoff volume (1 January 1995–31 December 1996).

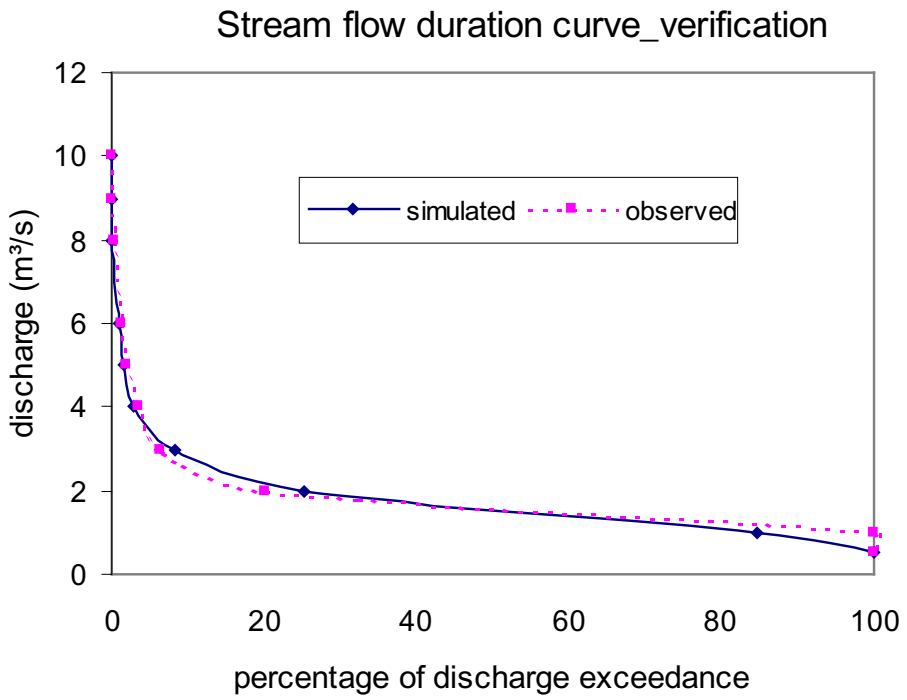

Fig. 12. Flow duration curves for the model verification results and the observed data.

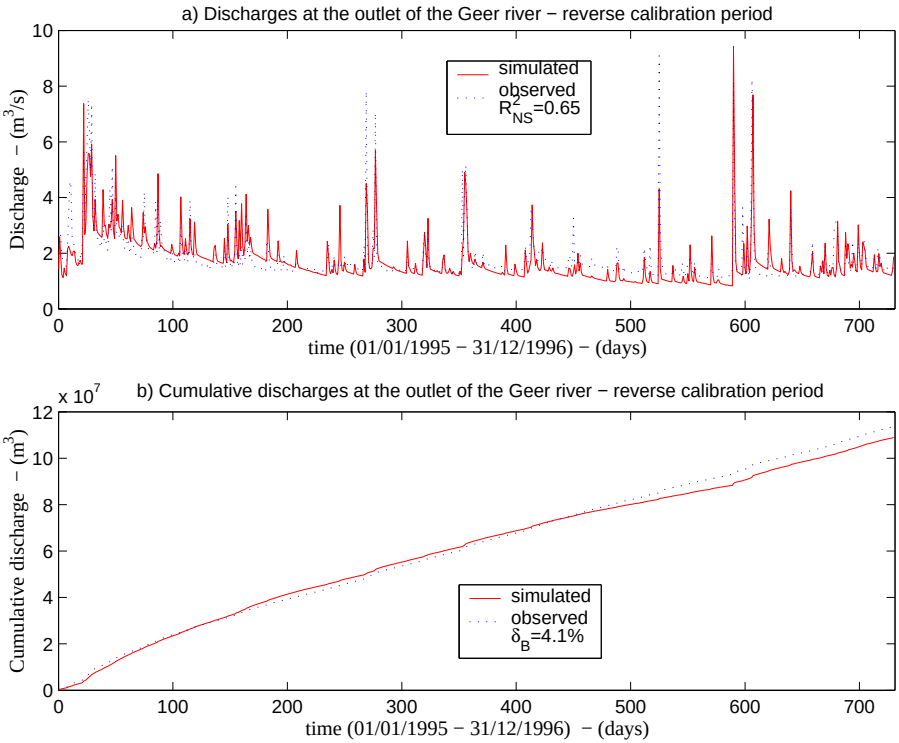

Fig. 13. Calibration results by reversing the calibration/verification periods (1 January 1995–31 December 1996): **(a)** observed and simulated discharge, **(b)** accumulated observed and simulated runoff.

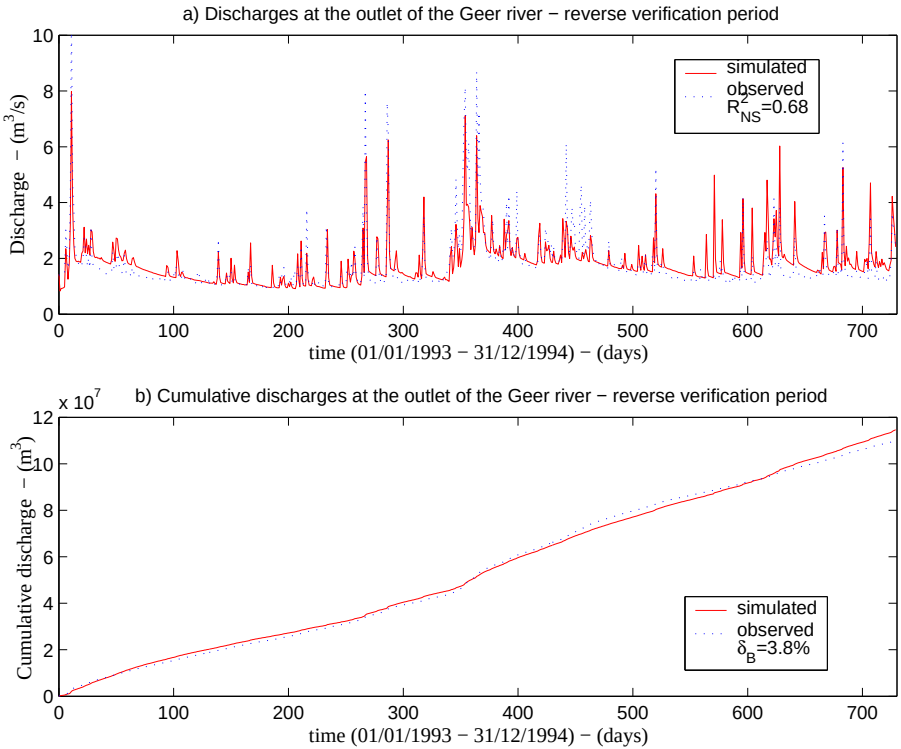

Fig. 14. Verification results by reversing the calibration/verification periods (1 January 1993–31 December 1994): **(a)** observed and simulated discharge, **(b)** accumulated observed and simulated runoff.